

Supplementary Information for

**Size control of zwitterionic polymer
micro/nanospheres and its dependence on sodium
storage**

*Shuming Zhuo, Mi Tang, Yanchao Wu, Yuan Chen, Shaolong Zhu, Qian Wang, Cong Xia and
Chengliang Wang**

School of Optical and Electronic Information, Wuhan National Laboratory for Optoelectronics
(WNLO), Huazhong University of Science and Technology, Wuhan, 430074, China

Synthesis of PPS

In a typical procedure, 6 mmol (0.415 mL) pyrrole and 6 mmol (0.684 g) squaric acid were dissolved in the 120 mL 1-butanol/ toluene (2:1) mixed solvent. The reaction mixture was stirred at 110 °C for 24 h. The precipitates were filtered and washed several times with 1-butanol, methanol and chloroform, successively. The residue was dried in a vacuum oven at 90 °C for 12 h, yielding 700 mg (71.5%) nanospheres of PPS-L. The other PPS micro/nanospheres were synthesized by using different amount or ratio of reactants and solvents (see details in Table 1 and Table S1) under the same procedure.

Material characterization and electrochemical measurements

FE-SEM images were obtained from a Gemini 300 (Zeiss) scanning electron microscope. XRD patterns were measured with a Cu-K α X-ray radiation source ($\lambda = 0.154056$ nm) incident radiation by a X'Pert3 Powder instrument. The BET were carried out on Agilent DD2 Belsorp-max within N₂ atmosphere. The Fourier transform infrared attenuated total reflection (FTIR-ATR) spectra were recorded in the range 400-4000 cm⁻¹ on a Bruker ALPHA spectrometer. XPS measurements were carried out on a ThermoFisher EscaLab 250Xi at a 58° angle of emission using a monochromatic Al K α source (E_{photon} = 1486.6 eV) with a 10 mA filament current and a 14.7 keV filament voltage source energy. The solid-state ¹³C magic angle spinning nuclear magnetic resonance (NMR) experiments were tested on Agilent DD2 NMR 400MHz NMR Spectrometer with one NMR probe.

All electrochemical tests were performed using 2032 coin cells assembled in Ar-filled glovebox. Na metal was used as anode and the electrolyte was 1 M NaPF₆ in dimethyl ether (DME). All the electrodes were made of a mixture of active materials, carbon black and polyvinylidene fluoride

(PVDF) binder in a weight ratio of 5:4:1. The slurry of electrodes in NMP was cast on Al foil and then placed in vacuum at 100 °C for 12 h. The mass loading of the active materials was about 1 mg cm⁻² for all the samples. The galvanostatic charge/discharge tests were conducted on a battery program-control test system (LANHE-CT2001A, Wuhan, China) in the voltage range from 1.2 to 3.5 V. Cyclic voltammetry (CV), electrochemical impedance spectroscopy (EIS) and galvanostatic intermittent titration technique (GITT) were performed on a BioLogic VSP potentiostat. CV measurements were recorded between 3.5 V and 1.2 V at different scan rates. EIS were collected at frequencies ranging from 100 MHz to 5 mHz. The GITT was employed at a pulse of 38 μA cm⁻² for 5 min and with 30 min interruption between each pulse. All above tests were performed at room temperature.

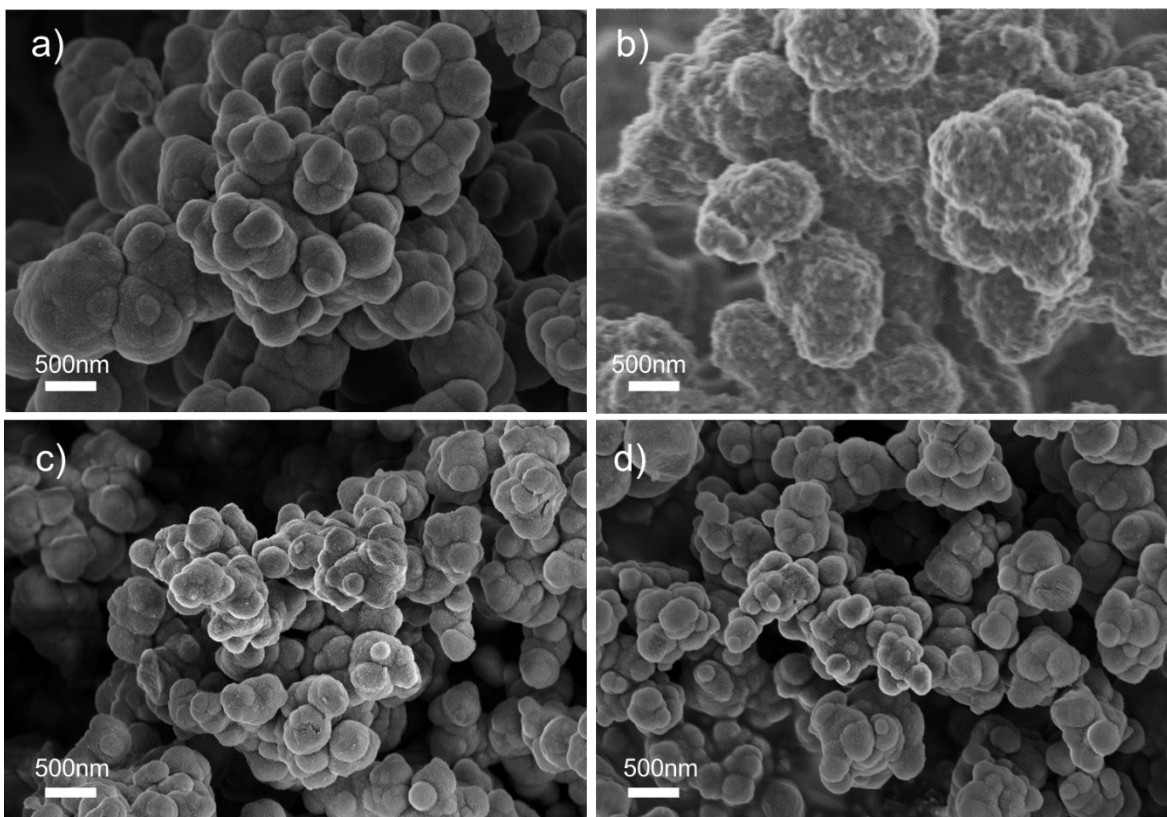


Fig. S1 SEM images of other PPS micro/nanospheres without regular shapes and uniform sizes (summarized in Table S1): a) sample 8, b) sample 9, c) sample 10, d) sample 11. All the magnifications are 20,000X. We also tested many other conditions, and all of them showed similar results. Therefore, only four samples are shown here as representatives.

Table S1 The comparison of other micro/nanospheres without regular shapes and uniform sizes and the corresponding experimental conditions. We also tested many other conditions, and all of them showed similar results. Therefore, only four samples are shown here as representatives.

Sample Index	Solvent ratio of 1-butanol and toluene	Concentration of reactants /mol L ⁻¹	Size/nm	Fig.
8	2:1	0.025	Aggregates of 300~500 nm particles	Fig. S1a
9	1:5	0.0125	Aggregates of 700~800 nm particles with rough surface	Fig. S1b
10	1:0	0.00625	Aggregates of 200~300 nm particles	Fig. S1c
11	1:0	0.025	Aggregates of 200~300 nm particles	Fig. S1d

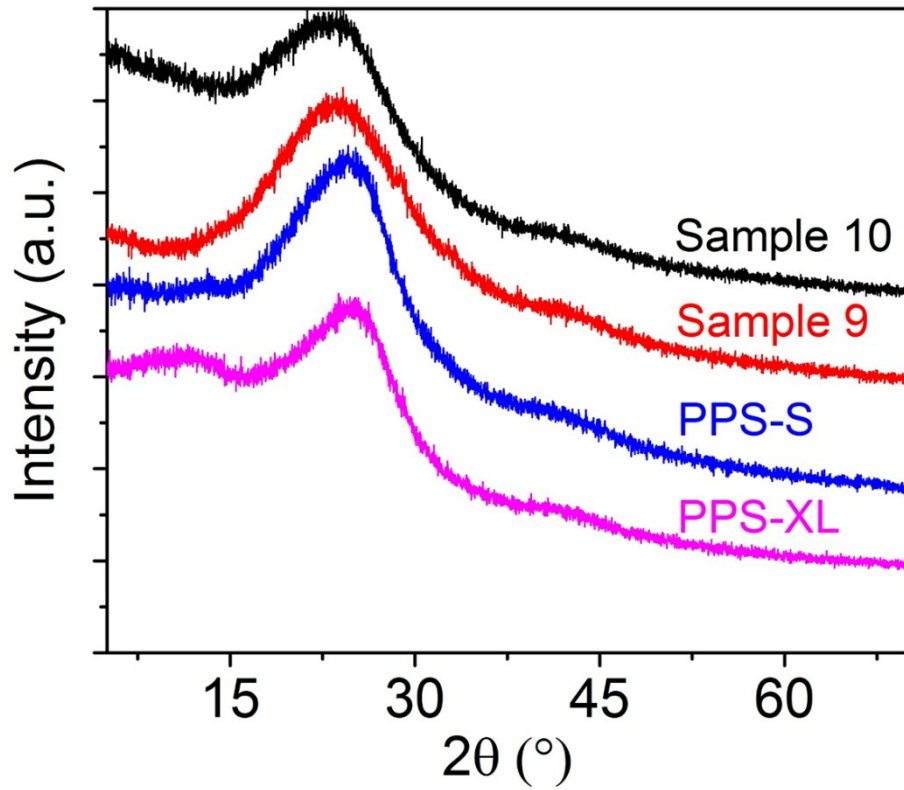


Fig. S2 Typical XRD patterns of PPS micro/nanospheres, showing only one broad peak which suggested that all the PPS with different morphologies were amorphous. Sample 2 (PPS-XL), 6 (PPS-S), 9 and 10 are presented as example.

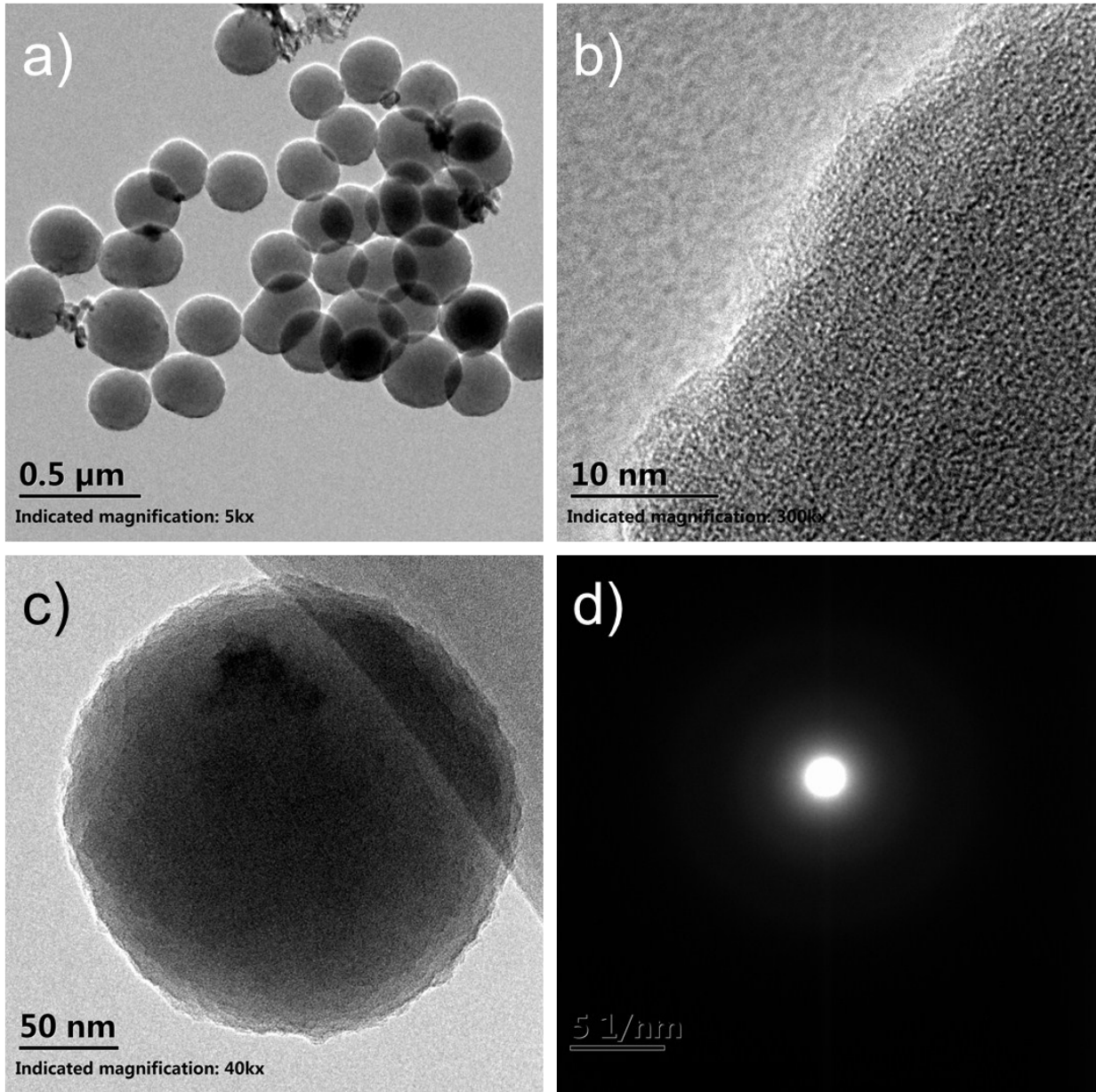


Fig. S3 (a-c) TEM images and (d) SAED patterns of PPS-XS, showing amorphous structure.

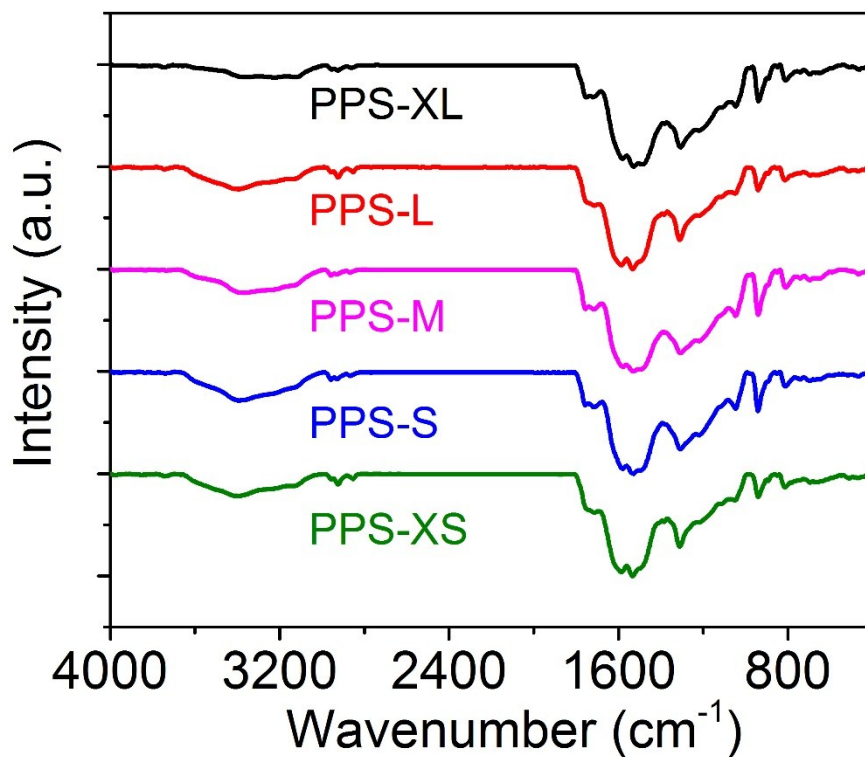


Fig. S4 FTIR spectra of five PPS micro/nanospheres (PPS-XL, PPS-L, PPS-M, PPS-S and PPS-XS). Normally, C=O stretching of 1,3-squarate is observed at lower frequency (around 1600 to 1620 cm^{-1}), while 1,2-squarate is noted by higher strong peaks (around 1730 to 1790 cm^{-1})¹. All the five samples showed weak adsorption around 1750 cm^{-1} and strong peaks around 1600 cm^{-1} , indicating the formation of 1,3-zwitterionic repeating units. These results are consistent with the previous reports²⁻⁶. No significant differences were observed between the five samples, which indicated that PPS micro/nanospheres with different particle sizes have the same chemical structures.

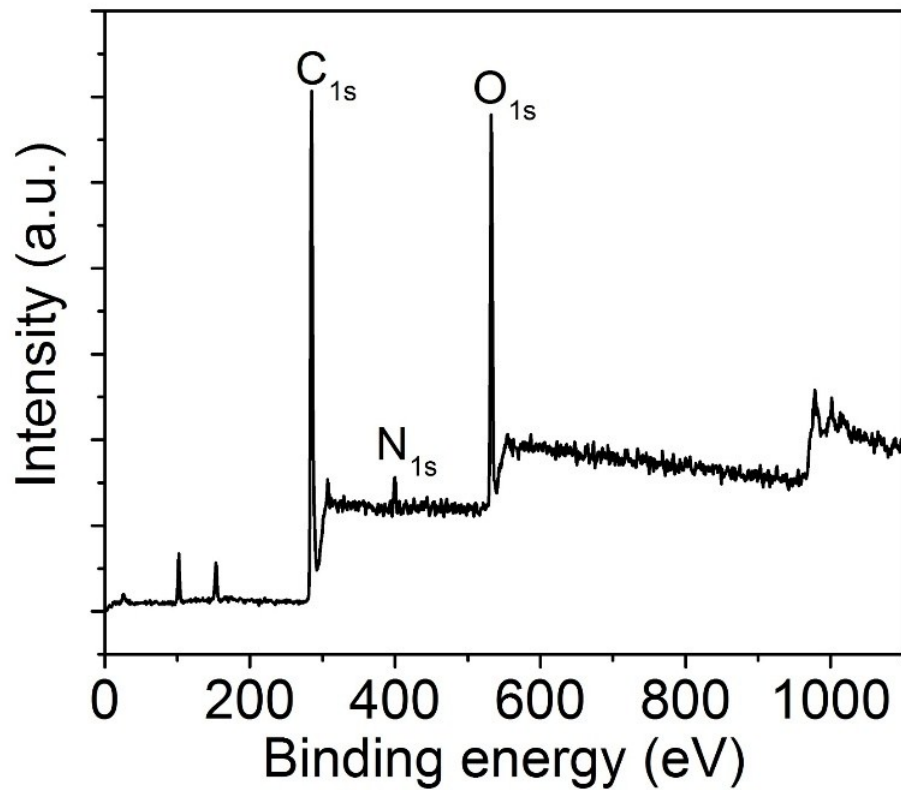


Fig. S5 Typical XPS spectra of PPS micro/nanospheres. Only C, O and N elements are observed in the PPS samples.

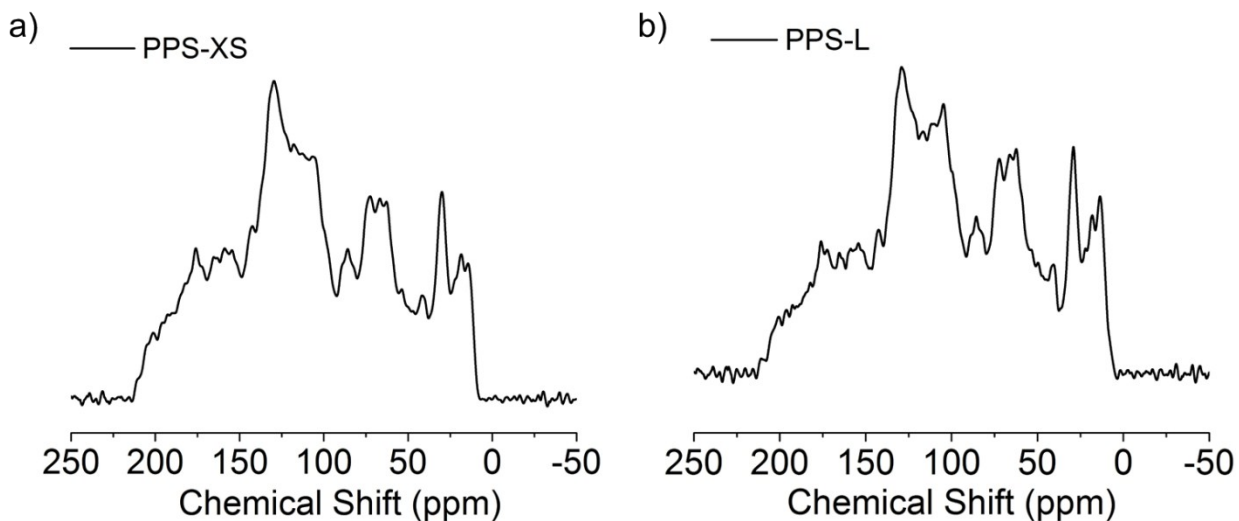


Fig. S6 Typical solid-state ^{13}C NMR spectra of PPS. a) PPS-XS and b) PPS-L micro/nanospheres are shown here as representatives. The peaks at around 176 ppm and 160 ppm affirmed the existence of the C=O and C-O bonds, corresponding to the carbon atoms in carbonyl groups. The strong peaks at 130 ppm and 118 ppm are assigned to the carbons on the pyrrole ring. The extra peaks at 60~70 ppm and 20~30 ppm can be identified to the carbons in butoxy groups of terminal squaraine units generated during the reaction⁷. No significant differences were observed between the two spectra, which indicated that PPS micro/nanospheres with different particle sizes have the same chemical structures.

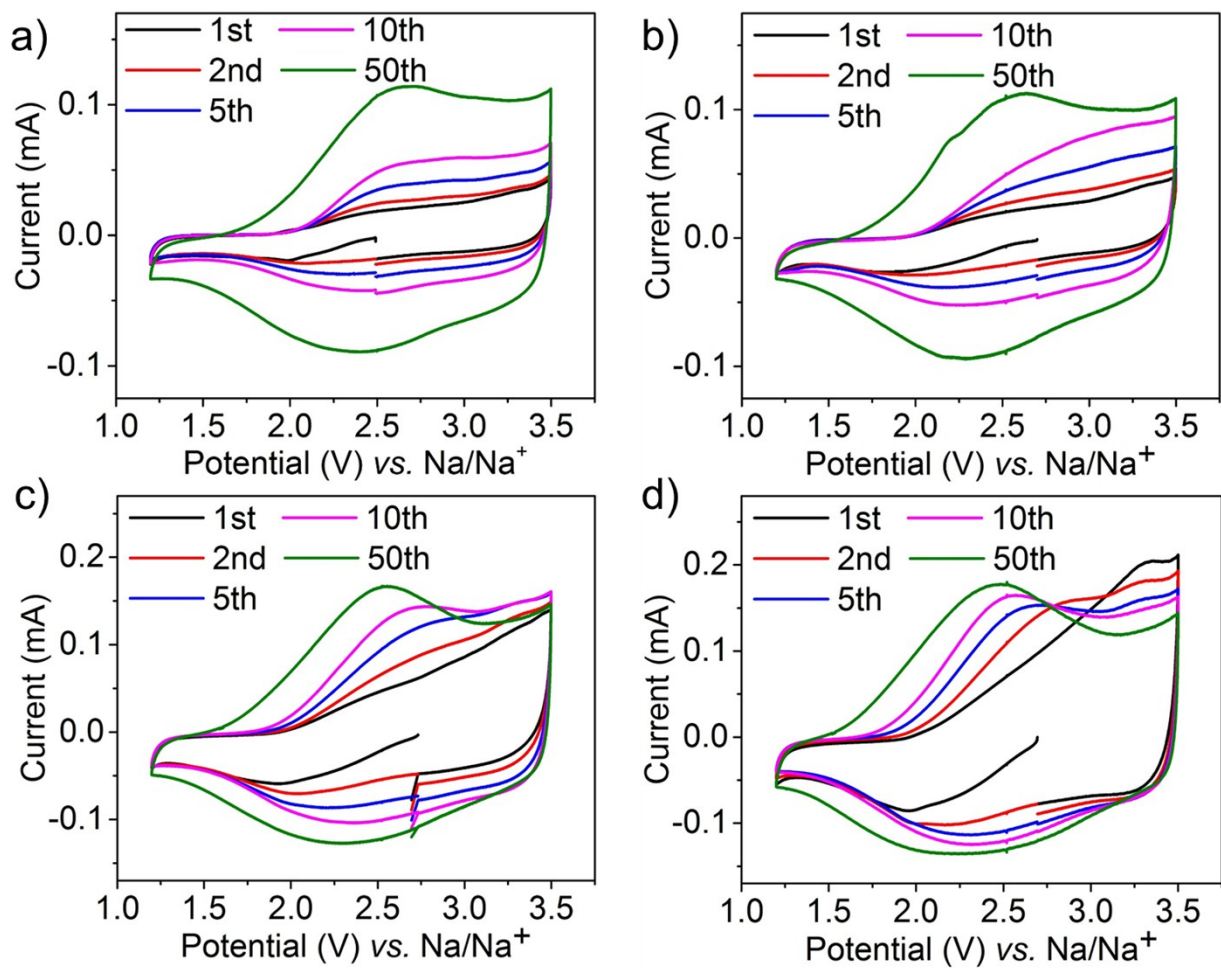


Fig. S7 Typical CV curves of PPS electrodes in OSIBs at a scan rate of 0.5 mV s^{-1} : a) PPS-XL, b) PPS-L, c) PPS-M and d) PPS-S.

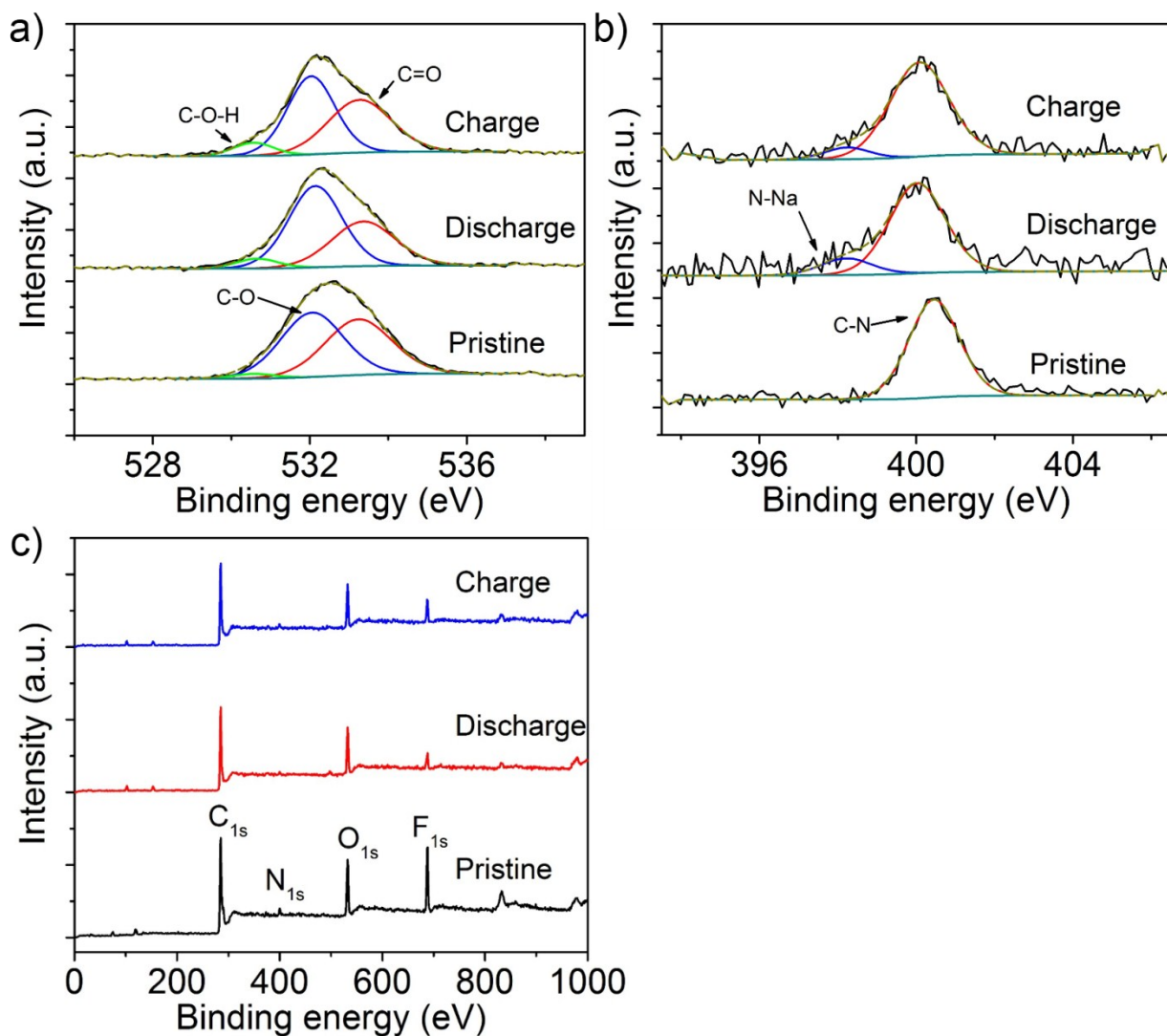


Fig. S8 XPS spectra of PPS electrodes (pristine, discharged to 1.2 V and charged to 3.5 V respectively): a) O 1s, b) N 1s and c) full range. According to the O 1s spectra, the signal of C=O double bonds (~ 533.3 eV) decreased and the signal of C-O single bonds (~ 532.0 eV) increased, after being fully discharged. The relative intensity of the two signals showed opposite variation after being fully charged. These results indicated the transformation between C=O double bonds and C-O single bonds during cycling⁸. Moreover, a weak peak at around 530.6 eV probably is associated with C-OH groups on the squaraine unit, suggesting the resonance structure from neutral carbonyl groups or C-OH groups to zwitterionic groups. From the N 1s spectra, a new peak

appeared at ~ 398.1 eV after being discharged, which probably can be ascribed to the acceptance of an electron and a sodium ions⁹. No obvious phosphorus peaks appeared in the XPS spectra of the charged electrode films, which indicated that there was no embedding of PF_6^- ions. All these results clearly proved that the storage mechanism of PPS involved the intercalation of cation (Na^+) rather than anion (PF_6^-). These results are coincident with the theoretical storage mechanism as shown in Scheme 1b.

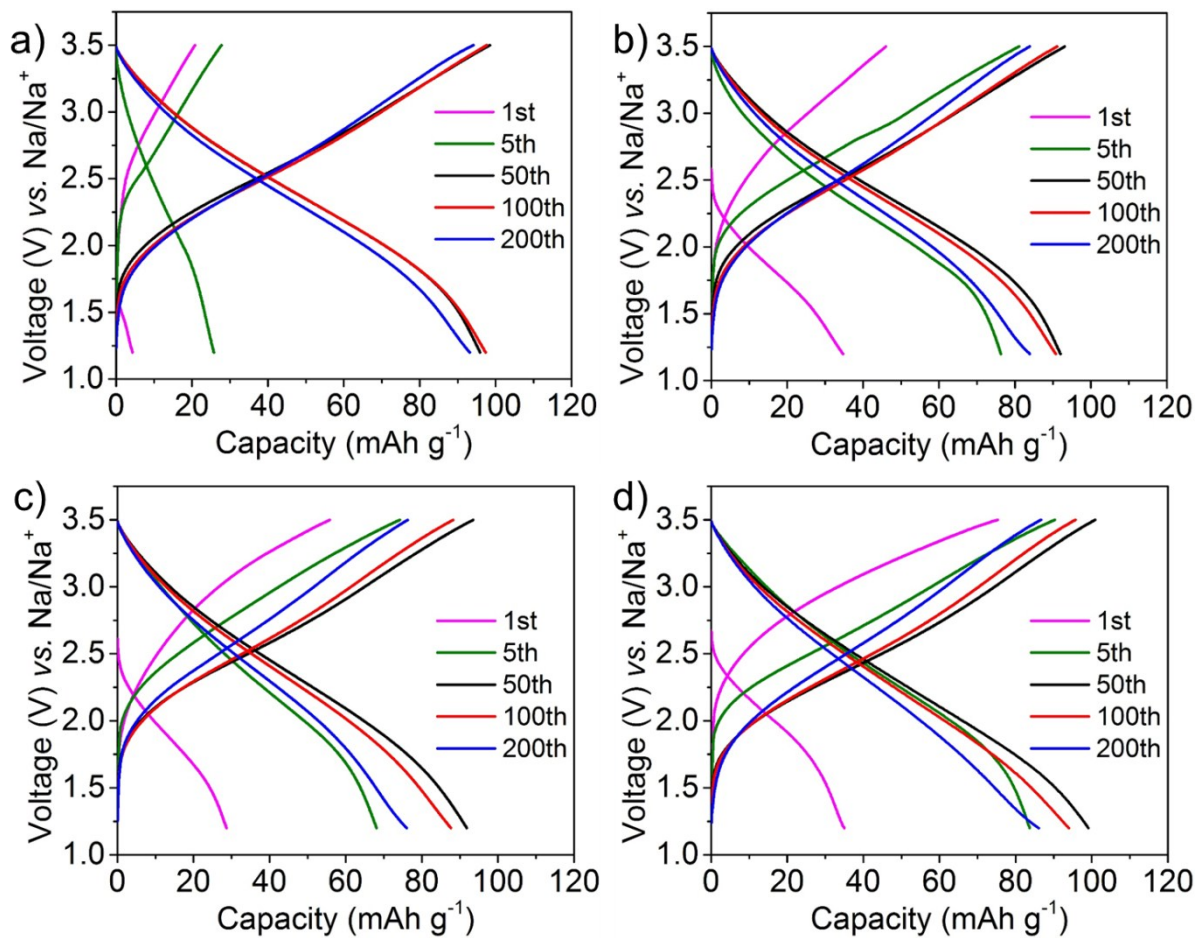


Fig. S9 Voltage profiles of PPS electrodes in OSIBs in the voltage range of 1.2-3.5 V at the rate of 50 mA g⁻¹: a) PPS-XL, b) PPS-L, c) PPS-M and d) PPS-S.

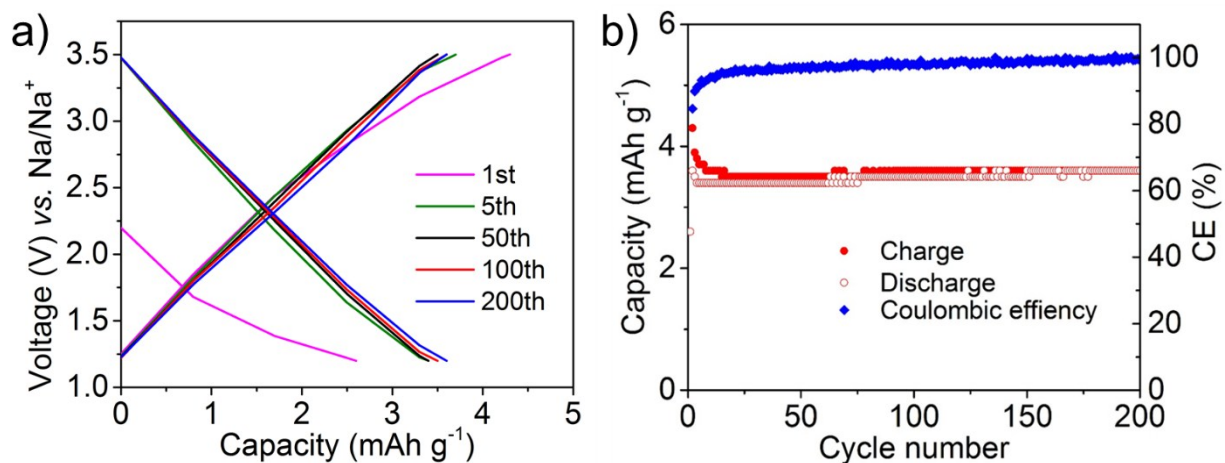


Fig. S10 Electrochemical performance of super-P at a current density of 50 mA g⁻¹. The electrodes were prepared by mixing super-P with polyvinylidene fluoride (PVDF) at a weight ratio of 4:1 in the presence of N-methyl-2-pyrrolidone (NMP), and then the mixture was coated on Al foil and dried at 100 °C overnight under vacuum conditions.

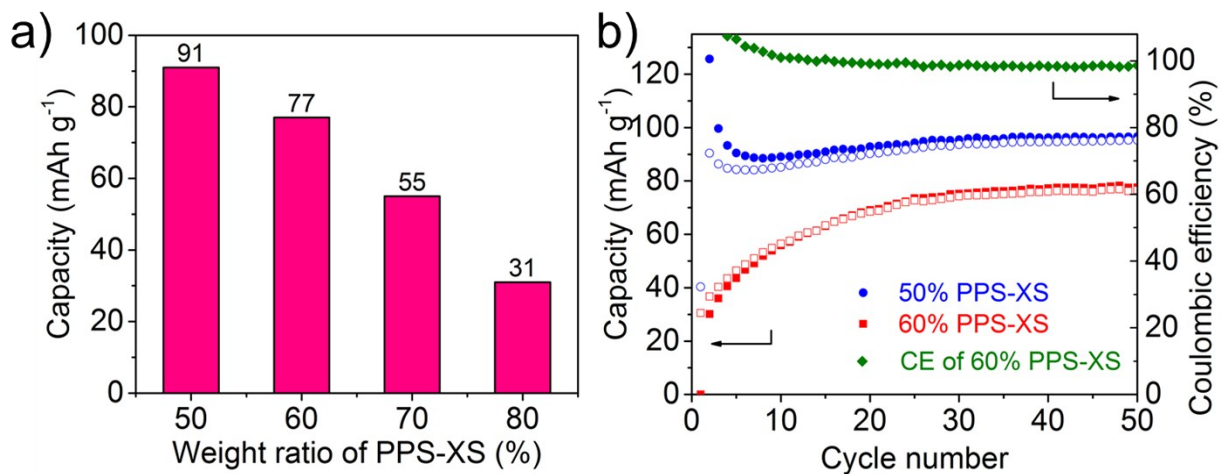


Fig. S11 The electrochemical performance by using different ratios of active materials. a) Capacity comparison of PPS-XS electrodes by using different ratios of active materials at a current density of 50 mA g⁻¹. b) Comparisons of the specific capacity and cycle stability with two ratios of active materials: 60% (red) and 50% (blue) at a current density of 50 mA g⁻¹.

Table S2 The Brunauer–Emmett–Teller (BET) specific surface areas of five PPS samples calculated from their N₂ sorption isotherm at 77 K. Basically, PPS samples with smaller micro/nanospheres had higher specific surface areas.

Materials	PPS-XL	PPS-L	PPS-M	PPS-S	PPS-XS
$a_{s,BET}/m^2 g^{-1}$	14.225	18.218	50.998	42.900	65.931

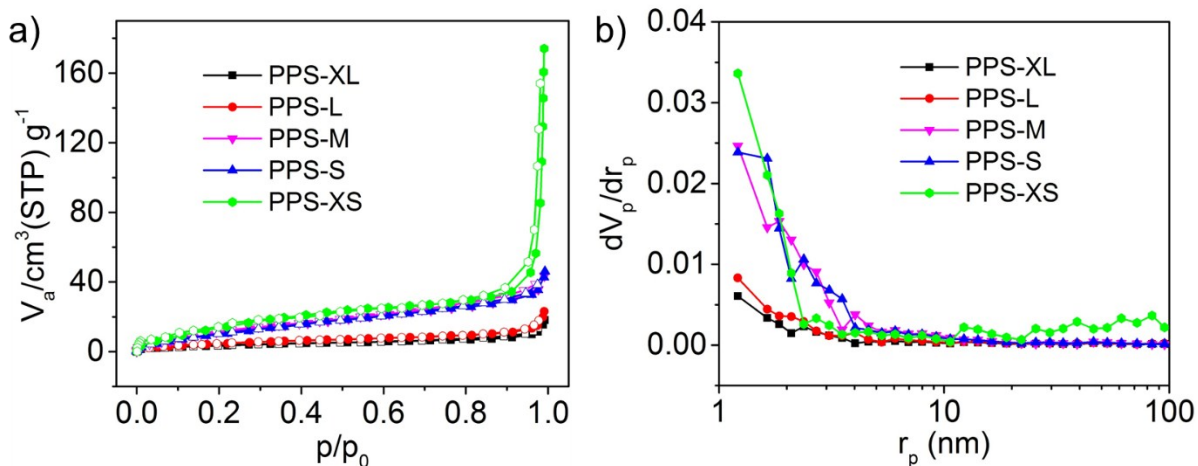


Fig. S12 a) N₂ adsorption (solid symbol) and desorption (open symbol) isotherm profile of five PPS micro/nanospheres and b) the corresponding pore size distribution of five PPS samples.

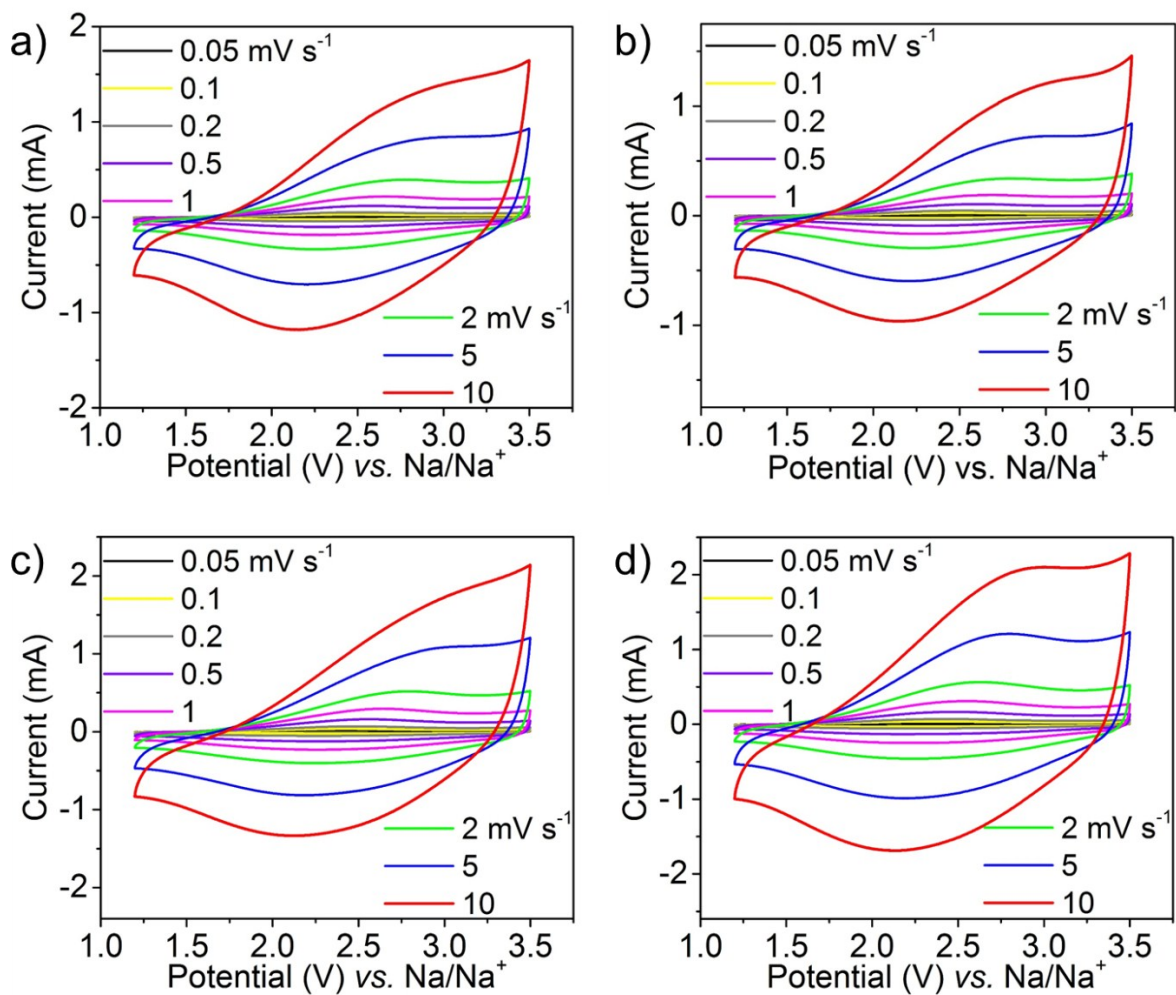


Fig. S13 CV curves of PPS electrodes at different scan rates (from 0.05 to 10 mV s⁻¹): a) PPS-XL, b) PPS-L, c) PPS-M and d) PPS-S.

Table S3 Slopes of every peak in the $\log i$ vs. $\log \nu$ plots in Fig. 3b.

	PPS-XL	PPS-L	PPS-M	PPS-S	PPS-XS
b-value (A)	0.86158	0.86327	0.87395	0.88311	0.88547
b-value (C)	0.88457	0.86268	0.86535	0.89537	0.92017

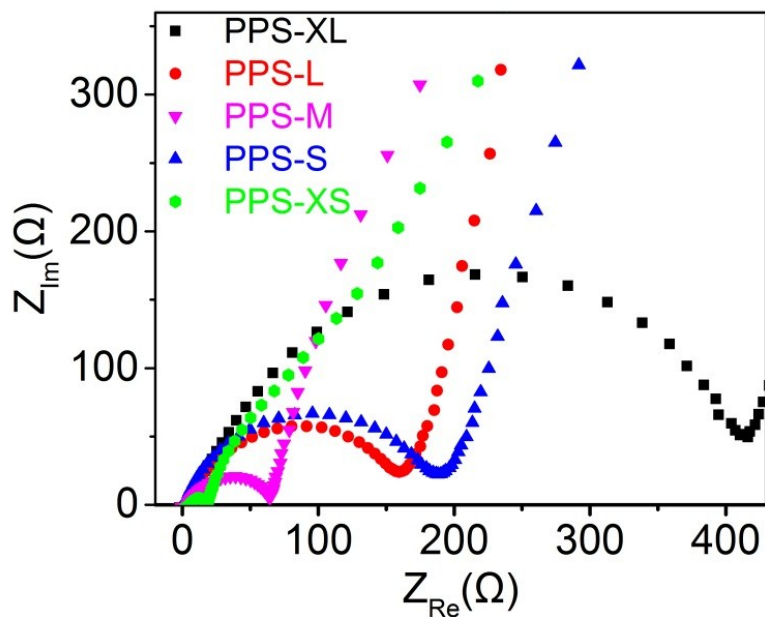


Fig. S14 EIS spectra of five PPS samples after the first discharge (corresponding parameters can be seen in Table S4).

Table S4 Parameters obtained from EIS data of PPS samples (Fig. S14).

Samples	PPS-XL	PPS-L	PPS-M	PPS-S	PPS-XS
R_{ct}/Ω	322	177	81	218	13
$\sigma_w/\Omega \text{ cm}^2 \text{ s}^{-0.5}$	1177.4010	957.8991	436.91579	603.52734	80.48433
$D/\text{cm}^2 \text{ s}^{-1}$	3.49E-16	6.98E-16	2.31E-15	1.21E-15	6.72E-14

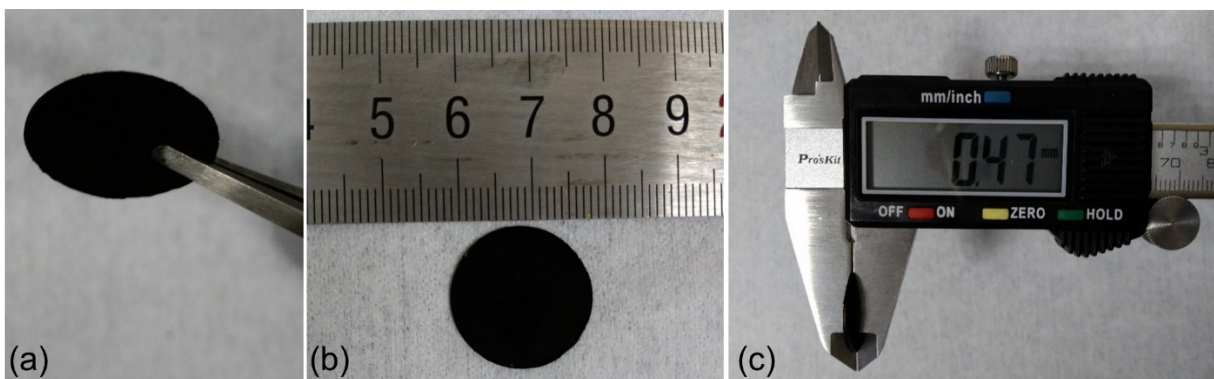


Fig. S15 Typical PPS pellets obtained by cold isostatic pressing (PPS-XL as an example)¹⁰. The molar volume (V_M) of every repeated unit was calculated by measured mass and the volume of every pressed PPS pellet. $C(\text{Na}^+)$ is the concentration of Na ions in the materials, which is calculated according to V_M .¹¹ The detailed results and the calculated V_M and $C(\text{Na}^+)$ of all the five samples are shown in Table S5.

Table S5 The calculated V_M and $C(\text{Na}^+)$ of all the five PPS samples.

Material	PPS-XL	PPS-L	PPS-M	PPS-S	PPS-XS
Thickness/cm	0.047	0.023	0.015	0.024	0.027
Diameter/cm	1.95	1.95	1.95	1.95	1.95
Weight/g	0.1131	0.0481	0.0316	0.065	0.0685
$V_M/\text{cm}^3 \text{ mol}^{-1}$	179.95	207.07	205.56	171.78	170.69
$C(\text{Na}^+)/\text{M}$	5.557	4.829	4.865	5.821	5.859

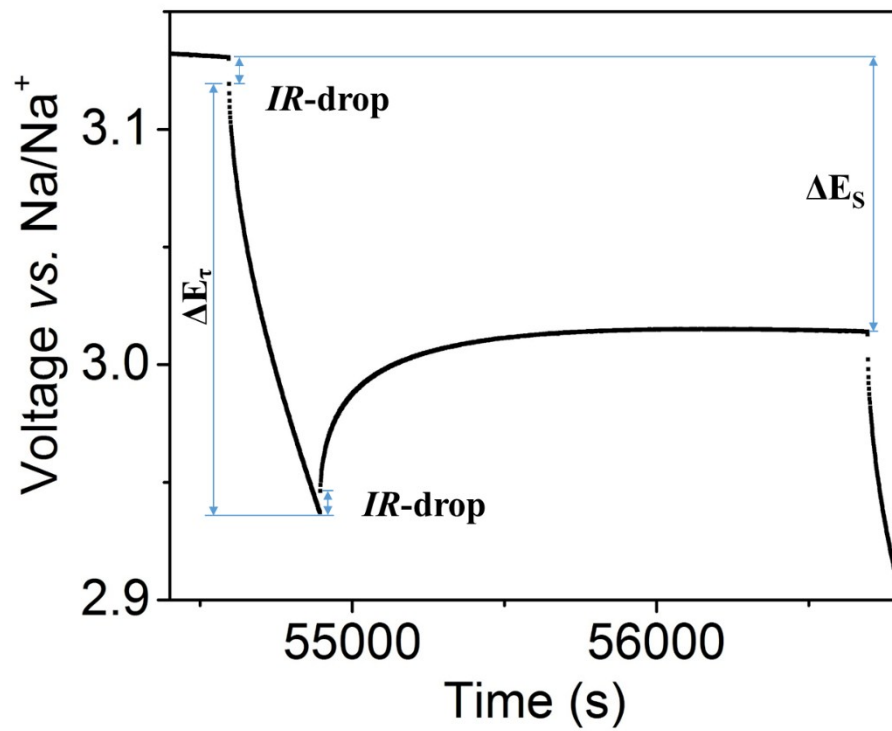


Fig. S16 GITT potential response curve with time for one typical step.

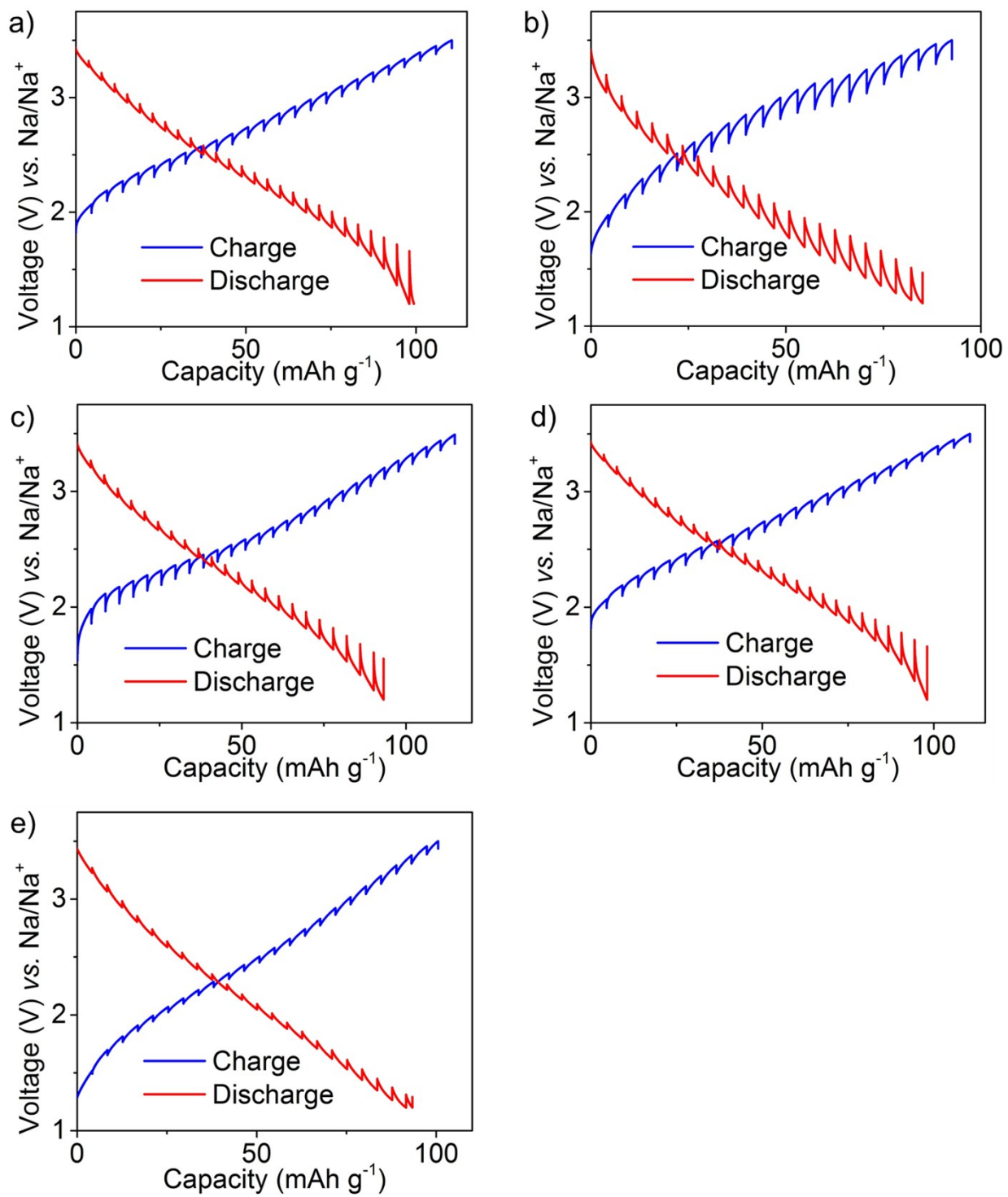


Fig. S17 GITT profiles of a) PPS-XL, b) PPS-L, c) PPS-M, d) PPS-S and e) PPS-XS.

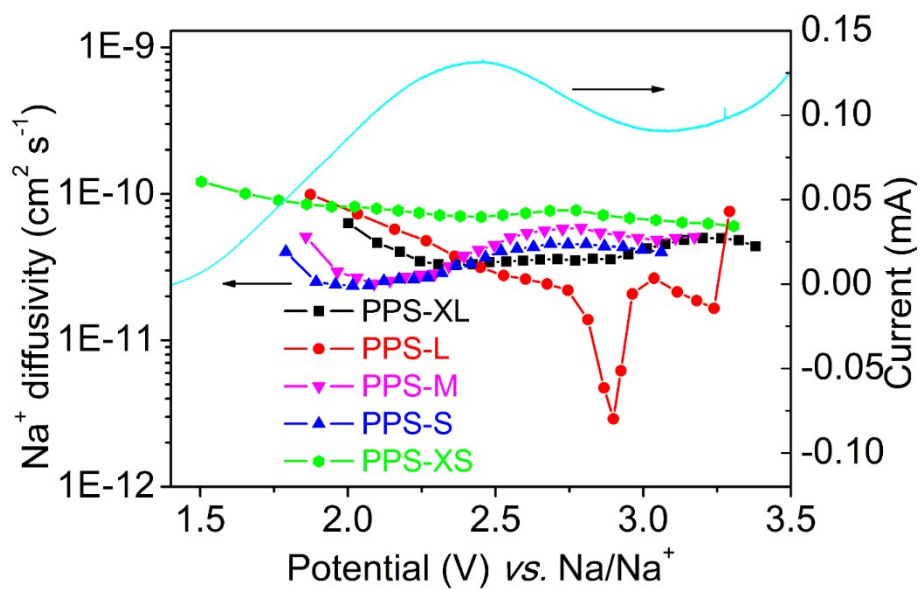


Fig. S18 Diffusivity of Na-ions during the charge process calculated from GITT methods versus potential. The CV curve (PPS-XS as an example) during anodic scan is also presented for comparison.

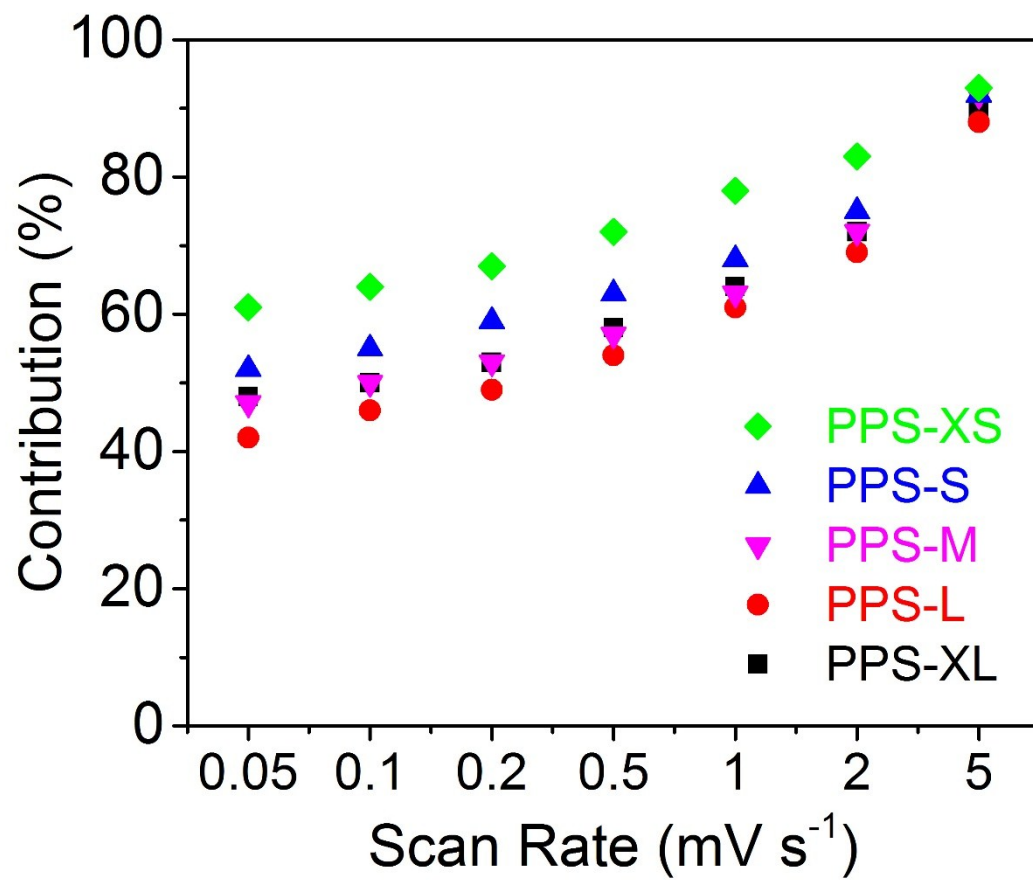


Fig. S19 The contribution of capacitive current at different scan rates (0.05, 0.1, 0.2, 0.5, 1, 2 and 5 mV s⁻¹).

REFERENCES

1. D. Lynch, *Metals*, 2015, **5**, 1349.
2. A. Ajayaghosh, C. R. Chenthamarakshan, S. Das and M. V. George, *Chem. Mater.*, 1997, **9**, 644-646.
3. D. E. Lynch, U. Geissler, I. R. Peterson, M. Floersheimer, R. Terbrack, L. Feng Chi, H. Fuchs, N. J. Calos, B. Wood, C. H. L. Kennard and G. John Langley, *J. Chem. Soc., Perkin Trans. 2*, 1997, 827-832.
4. C. R. Chenthamarakshan, J. Eldo and A. Ajayaghosh, *Macromolecules*, 1999, **32**, 5846-5851.
5. D. E. Lynch, U. Geissler, N. J. Calos, B. Wood and N. N. Kinaev, *Polym. Bull.*, 1998, **40**, 373-380.
6. D. E. Lynch, U. Geissler and K. A. Byriel, *Synth. Met.*, 2001, **124**, 385-391.
7. G. Xia and H. Wang, *J. Photochem. Photobiol., C*, 2017, **31**, 84-113.
8. C. Wang, Y. Fang, Y. Xu, L. Liang, M. Zhou, H. Zhao and Y. Lei, *Adv. Funct. Mater.*, 2016, **26**, 1777-1786.
9. M. V. Zeller and S. J. Hahn, *Surf. Interface Anal.*, 1988, **11**, 327-334.
10. M. Tang, S. Zhu, Z. Liu, C. Jiang, Y. Wu, H. Li, B. Wang, E. Wang, J. Ma and C. Wang, *Chem*, 2018, **4**, 2600-2614.
11. X. Wang, H. Hao, J. Liu, T. Huang and A. Yu, *Electrochim. Acta*, 2011, **56**, 4065-4069.